NANO LETTERS

2008
Vol. 8, No. 8
2469-2472

Nanohole Array as a Lens

Fu Min Huang,*,† Tsung Sheng Kao,† Vassili A. Fedotov,† Yifang Chen,‡ and Nikolay I. Zheludev†

Optoelectronics Research Center, University of Southampton, SO17 1BJ, United Kingdom, and Central Microstructure Facility, Rutherford Appleton Laboratory, Didcot, OX11 OQX, United Kingdom

Received May 23, 2008; Revised Manuscript Received June 6, 2008

ABSTRACT

We demonstrate that a quasi-crystal array of nanoholes in a metal screen can mimic a function of the lens: one-to-one imaging of a point source located a few tens of wavelengths away from the array to a point on the other side of the array. A displacement of the point source leads to a linear displacement of the image point. Complex structures composed of multiple point sources can be faithfully imaged with resolutions comparable to those of high numerical aperture lenses.

Nanohole arrays in metal screens have exhibited many interesting optical properties, most notably the extraordinary transmission of light through periodic[1] and quasi-periodic[2] nanoholes, polarization conversion[3] and optical energy concentration.[4,5] Recently, we have demonstrated that a quasi-periodic array of nanoholes in a metal screen can concentrate optical energy into hot spots and form subwavelength spots at distances a few tens of wavelengths away from the array,[4,5] when illuminated with plane waves (Figure 1a).

Here, we further demonstrate that such an array of quasi-crystal nanoholes in a metal screen can image a point source a few tens of wavelengths from the array into a spot on the other side of the array (Figure 1b). A displacement of the point source leads to a linear displacement of the image point; therefore, the array can perform a one-to-one imaging function like a conventional lens. We show that complex structures composed of multiple point sources can be faithfully imaged with resolutions comparable to those of conventional lenses with high numerical apertures. Such a nanohole array lens may find important applications in circumstances where conventional optical lenses are not readily applied, like X-ray imaging, nano-optical circuits, and so forth.

Although nearly any array of small holes will create a diffraction pattern of foci when illuminated by a point source, a careful choice of nanohole pattern is required for lensing applications. For instance, a regular 80 × 80 array of 200 nm holes (Figure 2a) will be self-imaged via the Talbot effect into a dense pattern of hot-spots and is not suitable as a lensing device (Figure 2c). However, a Penrose array of 200 nm holes (Figure 2b) can at some distances create an isolated

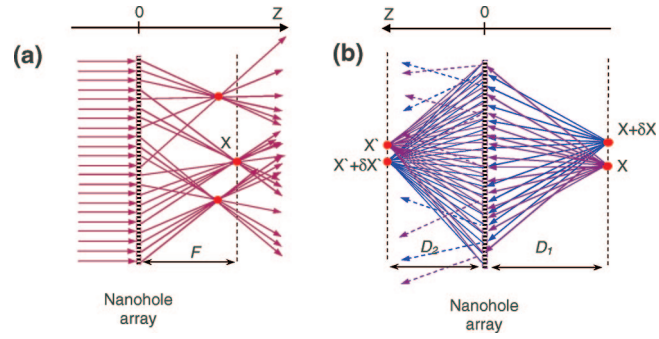

Figure 1. Schematic diagrams illustrating a quasi-periodic array of nanoholes as a light concentrator converting a plane wave into hot-spot foci (a) and performing the function of a lens imaging two closely spaced optical point-sources (x and $x + \delta x$) to two spots (x' and $x' + \delta x'$) on the other side of the array (b).

hot-spot of electromagnetic radiation as presented in Figure 2d. The case of a Penrose array of nanoholes as a lensing device will be investigated here in detail. In the examples given below, we will first investigate imaging of a point-like source on one side of the array into one of the foci on the other side of the array and will then consider imaging of an ensemble of point sources followed by providing an experimental verification of the concept.

The phenomenon of "lensing" by the nanohole array (mimicking a function of the conventional glass lens) results from the partial reconstruction of the array's field in the diffraction zone, in a manner analogous to the classical Talbot effect[6] observed with periodic grating illuminated with a plane wave, where diffraction leads to the reconstruction of the grating's field at periodic distances from the grating. In the Talbot effect, a grating with period a images itself at multiples of the Talbot distance $Z_T = a^2/\lambda$ when illuminated with a coherent plane wave. Montgomery[7] has shown that a

* Corresponding author.
† University of Southampton.
‡ Rutherford Appleton Laboratory.

10.1021/nl801476v CCC: $40.75
Published on Web 06/24/2008

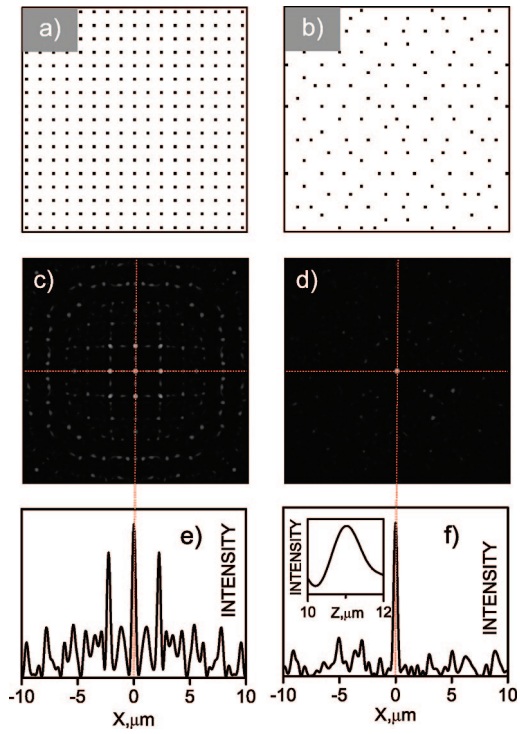

Figure 2. Regular (a) and quasi-crystal (b) arrays of holes and 20 $\times$ 20 μm^2 fragments of their diffraction patterns (c,d), respectively, at a distance $Z = 11$ μm from the array. (e,f) Scans across the patterns' centers. In both cases, a point light source with a wavelength $\lambda = 660$ nm is positioned at $Z = -11.4$ μm on the other side of the array. The inset to f shows the intensity of the hot-spot as a function of distance from the array.

wide range of patterns can image themselves, with linear periodic grating being only one example. A pattern will show full reconstruction at a distance Z if its spatial frequencies are discrete and located in the reciprocal plane at rings of radii $\rho^2 = 1/\lambda^2 - (m/Z)^2$, where m is an integer such that $0 \leq m \leq Z/\lambda$. For instance, circular or linear diffraction gratings are self-imaging objects whose spectra in the reciprocal lattice are sets of equidistant rings or dots, respectively. The spectrum of the quasiperiodic array lies somewhere between the dotted spectrum of a linear grating and the rings of a circular grating. However, as the rich spectrum of frequencies of the quasi-periodic array are located on circles (see, for instance, ref 4) the Montgomery condition is fulfilled for all spectral maxima, but not necessarily simultaneously. Therefore, the self-imaging distance will be different for different rings of maxima on the reciprocal lattice. Moreover, when a regular grating is illuminated with a divergent beam, for instance, created by a point-like source, the reconstructed image is magnified, so the reconstructed field does not necessarily have the same dimensions as the original pattern. Similarly, when partial reconstruction of the quasi-periodic array takes place, the pattern of reconstructed hot-spots has the appearance of a scaled partial image of the array. Thus, reconstruction of a quasi-periodic array of holes is a complex diffraction process which may be envisaged as a superposition of a large number of partial reconstructions happening at different heights at the array. With varying distance Z from the array, one will see a continuous evolution of partially reconstructed images of the array.

What is important, however, is that at some distances a pattern of well-defined sparsely distributed foci is seen resembling that of the focus of a conventional lens. The foci pattern results from a constructive interference of waves emanated from a large number holes in the array. As with focusing by a conventional lens, the focal spot size depends on the available wave vectors of the interfering waves, that is, on the solid angle from which the interfering waves area comes with larger solid angles giving better focusing. For the foci located at distances of a few wavelengths from the array, the number of constructively interfering waves coming from nearly a half-space solid angel is high, providing for a tight focusing. For a plane wave illumination, the pattern of foci is infinite, while in the case of a point-like source the pattern is brightest in that area on the other side of the grating which is immediately opposite the point source. If the grating is moved with respect to the point-like source along the direction perpendicular to axis Z, the pattern will move accordingly (Figure 1b) to maintain the constructive interference necessary for the formation of foci and thus mimicking a function of the conventional lens.

The nanohole array investigated in this work had a Penrose-like quasi-periodic pattern of approximate 10-fold symmetry formed by 200 nm square holes, with the minimum separation between neighboring holes of 1.2 μm. The array contained about 14 000 holes and had an overall size of about 200 $\times$ 200 μm^2. The hole pattern was designed according to algorithm described in ref 8.

The lensing properties of the quasi-crystal nanohole array were modeled using the Rayleigh−Sommerfeld scalar integration technique.[9,10] This technique has proved to be consistent with boundary conditions when the observation points approach the diffraction aperture and is therefore suitable for our analysis. In all of our calculations, we assume that the object plane is located at a distance $z = -11.4$ μm from the plane of the array.

Figure 3 shows characteristic different diffraction patterns created on one side of an array by a point source on the other side at different distances "Z" from the array. As the distance to the array varies, the diffraction pattern evolves dramatically, with a bright spot seen at the center of the image for some values of Z. This bright spot can be used as the "focus of a lens", and in this sense, two parameters are important, the spot diameter at half-height d and the diameter D of the "field of view" which we define as the dark area around the hot-spot where the intensity is less than $1/e$ of the peak intensity at the "focus". For lensing applications, one would like to minimize the focus d and maximize the field of view D.

From Figure 3, one can see that the Penrose array can generate subwavelength hot-spots with various fields of view. For instance, with coherent illumination at a wavelength of $\lambda = 660$ nm, at $Z = 5$ μm and $Z = 18$ μm, foci with diameters of 360 nm are generated with fields of view of 2.8 μm and 2.4 μm, respectively. A spot with a diameter as small as 200 nm can be generated within a smaller field of

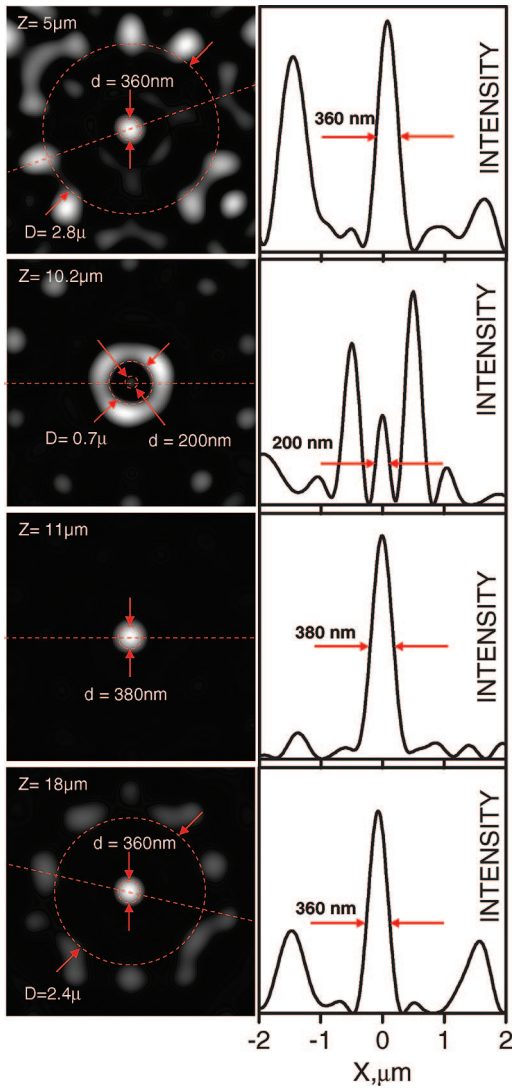

Figure 3. Foci created at different distances Z from a Penrose nanohole array illuminated by a point source with $\lambda = 660$ nm positioned at $z = -11.4$ μm. The dashed circles show "fields of view" and diameters of the foci.

view (Figure 3, $Z = 10.2$ μm), confirming that subwavelength optical fields can be created in the far field without evanescent waves.[4,5] The largest field of view, exceeding $D = 20$ μm, was found at $Z = 11$ μm where the focus diameter was 380 nm. The inset to Figure 2f shows the dependence of light intensity on the distance from the array of the $Z = 11$ μm focus. From here, one can estimate that the depth of focus (focal "waist") is 0.9 μm.

An essential property of a lens is the ability to image a point source and to distinguish between two neighboring points. This is illustrated in Figure 4. When the point source is moved within the object plane at $Z = -11.4$ μm from a starting position at $Y = 0$ to $Y = 400$ nm, the image spot moves linearly in the opposite direction in the image plane at $z = 11$ μm from $Y' = 0$ to $Y' = 400$ nm, in a manner analogous to a conventional lens with approximately unitary magnification (see Figure 4, upper row).

The imaging of two closely spaced point sources is illustrated for cases of both coherent and incoherent sources.

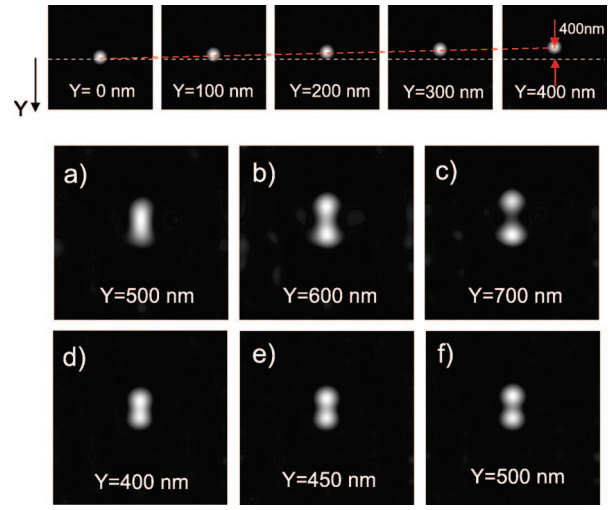

Figure 4. Lensing properties of the Penrose nanohole array. The series of images in the upper row shows one-to-one imaging of a single point source as it is translated in the Y direction in the object plane. Its image moves linearly in the image plane in the opposite direction. (a−c) Images of two coherent 660 nm optical point sources separated by $Y = 500$, 600, and 700 nm, respectively. (d−f) Images of two incoherent sources separated by $Y = 400$, 450, and 500 nm, respectively. The optical point sources are positioned at $z = -11.4$ μm, and the image spots are in the image plane at $z = 11$ μm. In all cases, the image size is 4×4 μm^2.

Figure 4a−c shows images of coherent sources separated by 500, 600, and 700 nm, respectively, while Figure 4d−f shows images of incoherent sources separated by 400, 450, and 500 nm. It appears that, as with a conventional lens, the resolving power of a nanohole array lens is better for incoherent illumination: according to the Rayleigh resolution criteria, coherent 660 nm point sources are resolved when spaced by 600 nm, while incoherent point sources are resolved by a separation of 450 nm. This may be compared with a conventional lens for which the coherent illumination resolution depends on numerical aperture NA and is given by $0.77\lambda/NA$.[11] Thus, the nanohole array shows a resolving ability analogous to a conventional lens with $NA = 0.85$ for coherent illumination. Similarly, the resolution of a conventional lens for incoherent illumination is given by $0.61\lambda/NA$,[11] and in this case, the Penrose array has an effective numerical aperture of 0.89.

The task of imaging a real object is illustrated in Figure 5 where we present images of multiple point sources of equal intensity of various configurations. The red dots indicate the expected positions of individual point sources images. The top row shows the case of coherent illumination while the bottom row shows that of incoherent illumination. The distances between points are $AB = 600$ nm, $AC = 700$ nm, $AD = 1000$ nm, $AE = 1140$ nm, $AF = 1000$ nm, and $EF = 420$ nm; the source wavelength $\lambda = 660$ nm. One can see that, under incoherent illumination, multiple point sources are faithfully imaged within a resolution of about 450 nm. In the case of coherent illumination, as with a conventional lens, the resolution is degraded somewhat because of interference effects between different sources.

Finally, we have experimentally demonstrated the lensing function of the nanohole array with a single point-like source.

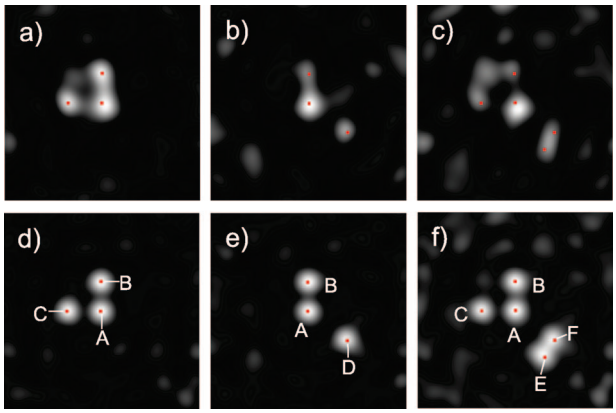

Figure 5. Images of complex objects created by multiple point sources. The top row (a−c) shows images under coherent illumination while the bottom row (d−f) corresponds to incoherent source imaging. All images are 4 × 4 μm^2.

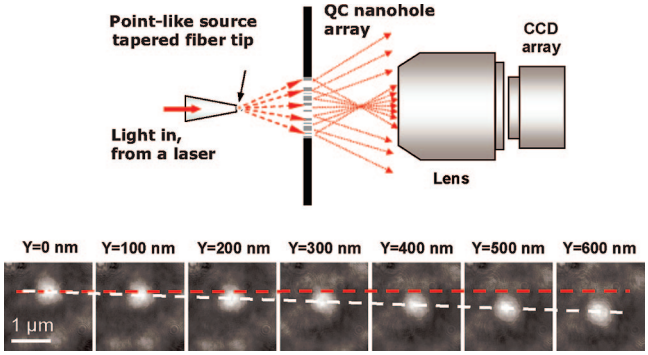

Figure 6. Schematic diagram of experimental setup. A tapered fiber is used as a point-like light source to illuminate the quasi-periodic nanohole array. The diffraction patterns at the other side of the array are imaged by a CCD array. A series of the CCD array images shows a motion of the hot-spot corresponding to the light source moving along the *Y* direction.

The array was manufactured by electron beam lithography in a 100 nm aluminum film deposited on a silica substrate to the same design as that used in the calculation. Our experimental setup is schematically illustrated in Figure 6. A metal coated tapered fiber of a scanning near-field optical microscope probe with an aperture of ∼100 nm was positioned above the nanohole array at a distance of Z = 11.5 μm. A diode laser operating at λ = 635 nm was launched into the fiber thus creating a point-like source near the nanohole array. The hot-spot pattern at the other side of the array was imaged onto the CCD array of a digital camera through an objective lens (NA = 0.65) and a magnifying lens in front of the camera. A pattern resembling that presented in Figure 2d and Figure 3 (third image from the top) was observed at $Z \simeq 11$ μm from the array. We have also observed the main lensing feature: when the point source (tapered fiber) moves, the image spot moves linearly in the opposite direction, as has been demonstrated by simulations shown in Figure 4.

In summary, we have demonstrated that a quasi-periodic array of nanoholes can perform the function of a lens, that is, the one-to-one imaging of a point source close to the array to an image on the other side of the array. Complex structures composed of multiple point sources can be faithfully imaged with resolutions comparable to those of high numerical aperture lenes. An interesting question emerges of whether lensing function ability with a resolution better than that of a conventional lens with a numerical aperture NA = 1 could be achieved with a hole array. Although the Penrose hole array can create subwavelength foci as small as 200 nm in diameter (see Figure 3), the field of view is not sufficiently large for practical imaging applications. However, superoscillation theory specifies[12] that no principal limitation exists on the size of hot-spots or on the field of view. We therefore argue that our results provide an encouraging indication that more sophisticated nanohole patterns could generate small subwavelength hot-spots with large fields of view, mimicking functions of true lenses.[13] Here, the price to pay for high resolution in a large field of view will be a decrease in the power concentrated in the hot-spot relative to the power going into the unfocused side-bands located outside the field of view.[14]

Acknowledgment. The authors would like to acknowledge the financial support of the EPSRC (U.K.) and fruitful discussions with E. Yablonovitch, N. Engheta, M. Denis, and F. J. Garcia de Abajo. The authors thank Kevin MacDonald for help in preparing the manuscript.

References

(1) Ebbesen, T. W.; Lezec, H. J.; Ghaemi, H. F.; Thio, T.; Wolff, P. A. *Nature* **1998**, *391*, 667–669.
(2) Papasimakis, N.; Fedotov, V. A.; Schwanecke, A. S.; Zheludev, N. I.; Garcia de Abajo, F. J. *Appl. Phys. Lett.* **2007**, *91*, 081503.
(3) Krasavin, A. V.; Schwanecke, A. S.; Reichelt, M.; Stroucken, T; Koch, S.; Wright, E. M.; Zheludev, N. I. *Appl. Phys. Lett.* **2004**, *86*, 201105.
(4) Huang, F. M.; Chen, Y.; Garcia de Abajo, F. J.; Zheludev, N. I. *Appl. Phys. Lett.* **2007**, *90*, 091119.
(5) Huang, F. M.; Chen, Y.; Garcia de Abajo, F. J.; Zheludev, N. I. *J. Opt. A: Pure Appl. Opt.* **2007**, *9*, S285−S288.
(6) Patorski, K. *Progress in Optics* **1989**, *27*, 3.
(7) Montgomery, W. D. *J. Opt. Soc. Am.* **1967**, *57*, 772.
(8) Lord, E. A.; Ramakrishnan, K.; Ranganathan, S. *Bull. Mater. Sci.* **2000**, *23*, 119–123.
(9) Wolf, E.; Marchard, E. W. *J. Opt. Soc. Am.* **1964**, *54*, 587–594.
(10) Gillen, G. D.; Guha, S. *Am. J. Phys* **2004**, *72*, 1195–1201.
(11) Born, M.; Wolf, E. *Principles of Optics*.
(12) Berry, M.; Popescu, S. *J. Phys. A: Math. Gen.* **2006**, *39*, 6965–6977.
(13) Zheludev, N. I. *Nat. Mater.* **2008**, *7*, 420–422.
(14) Frieden, B. R. *Opt. Acta* **1969**, *16*, 795–807.

NL801476V